Chinese Journal of Oceanology and Limnology
Vol. 35 No. 4, P. 792-802, 2017
http://dx.doi.org/10.1007/s00343-017-6023-7

Improvement of *Nannochloropsis oceanica* growth performance through chemical mutation and characterization of fast growth physiology by transcriptome profiling*

LIANG Sijie (梁思杰)[1, 2], GUO Li (郭栗)[1, 2], LIN Genmei (林根妹)[1, 2], ZHANG Zhongyi (张忠义)[1, 2], DING Haiyan (丁海燕)[1, 2], WANG Yamei (王亚梅)[1, 2], YANG Guanpin (杨官品)[1, 2, 3, **]

[1] *Laboratory of Marine Genetics and Breeding*, *Ocean University of China*, *Qingdao 266003*, *China*

[2] *College of Marine Life Sciences*, *Ocean University of China*, *Qingdao 266003*, *China*

[3] *Institutes of Evolution and Marine Biodiversity*, *Ocean University of China*, *Qingdao 266003*, *China*

Received Jan. 27, 2016; accepted in principle Apr. 25, 2016; accepted for publication Jun. 13, 2016

Abstract *Nannochloropsis oceanica* promises to be an industrial-level producer of polyunsaturated fatty acids. In this study, the fastest and slowest growing *N. oceanica* mutants were selected through N-methyl-N'-nitro-N-nitrosoguanidine mutation, and two mutant strains and the wild type (WT) subjected to transcriptome profiling. It was found that the OD_{680} reads at stationary growth phase of both WT and its mutants were proportional to their cell density, thus indicating their division rate and growth speed during culture. This chemical mutation was effective for improving growth performance, and the fast strain divided faster by upregulating the expression of genes functioning in the cell cycle and downregulating genes involved in synthesis of amino acids, fatty acids, and sugars as well as the construction of ribosome and photosynthetic machinery. However, the relationship among the effected genes responsible for cell cycle, metabolism of fatty and amino acids, and construction of ribosome and photosynthetic machinery remained unclear. Further genetic studies are required for clarifying the genetic/metabolic networks underpinning the growth performance of *N. oceanica*. These findings demonstrated that this mutation strategy was effective for improving the growth performance of this species and explored a means of microalgal genetic improvement, particularly in species possessing a monoploid nucleus and asexual reproduction.

Keyword: *Nannochloropsis oceanica*; mutation; cell cycle; transcriptome

1 INTRODUCTION

The development of environmentally friendly bioenergy is in increasing demand as it has been predicted that fossil fuels will be exhausted in the foreseeable future (Tilman et al., 2009). Microalgae, the primary producers of diverse ecological systems, grow rapidly and have the potential to afford significant industrial biomass and biofuel yields (Wijffels and Barbosa, 2010). Unfortunately, it is far from reality for microalgae to produce biofuel directly (Petkov et al., 2012). One restriction on biofuel biosynthesis is the lack of elite microalgal varieties. Early research has mainly focused on the isolation and tentative culture of biofuel-producing microalgae (Ortiz-Marquez et al., 2013); however, neither domestication nor genetic improvement of these microalgae has been initiated. It can be realistically expected that effective methods for improving terrestrial crops will function well in microalgae (Chepurnov et al., 2011). Actually, various strategies have indeed been applied for microalgal genetic improvement. To date, protoplast fusion (Tjahjono et al., 1994), genetic transformation (Kawata et al., 1991; Xue et al., 2015), chemical mutation (Zhang and Lee, 1997), atmosphere and room temperature

* Supported by the National Natural Science Foundation of China (No. 31270408) and the National High Technology Research and Development Program of China (863 Program) (No. 2014AA022001)
** Corresponding author: yguanpin@ouc.edu.cn

plasma (ARTP) mutation (Fang et al., 2013), genetic engineering (Ortiz-Marquez et al., 2013), selective breeding after genome shuffling (Takouridis et al., 2015), and diverse molecular techniques, such as genome editing, knocking-out, and knocking-down (Jinkerson and Jonikas, 2015), have been attempted in microalgae. Among these diverse methods for genetic improvement, both chemical and physical mutations have contributed significantly to crop breeding and performance. Such contributions have also been realized in microalgae, as in *N*-methyl-*N*'-nitro-*N*-nitrosoguanidine (MNNG) mutated *Chlorococcum* sp. that possess a two-fold higher astaxanthin content (Zhang and Lee, 1997). However, mutation techniques have not advanced genetic improvement of microalgae as a group of organisms, and the new tools are not available for nonmodel and in-culture microalgae. The yield of biomass (or growth speed), accumulation of desirable materials, and resistance to diverse stresses are the most important microalgal traits desirable for large-scale culture. Unfortunately, studies regarding these traits are scarce.

With the popularization of next-generation sequencing technology, transcriptome profiling has evolved into a routine approach to decipher the physiogenetic mechanisms of desirable traits of animals, plants, and microorganisms, including microalgae (Mardis, 2008; He et al., 2012). For example, transcriptome analysis has provided insights into C4-like photosynthesis and the oil body-forming mechanism in *Myrmecia incise* (Ouyang et al., 2013), the adaptation mechanisms of polar *Chlamydomonas* sp. (Kim et al., 2013) and *N. oceanica* (Guo and Yang, 2015), and the oil accumulation mechanisms of *Chlorella protothecoides* (Gao et al., 2014) and *Neochloris oleoabundans* (Rismani-Yazdi et al., 2012). However, such approaches have been little applied to unveiling the physiological processes and genetic mechanisms of the growth performance of microalgae.

The microalga *Nannochloropsis oceanica* possesses the potential for being a biofuel synthesizer (Boussiba et al., 1987; Sukenik et al., 1989). This species is known to be monoploid and asexual (Pan et al., 2011) and is thus suitable for modification of both its nuclear and cytoplasmic genes through mutation. Among currently available mutation methods, chemical mutation is the most convenient. As a preliminary study in this laboratory, *N. oceanica* was mutated chemically with MNNG. From the resulting mutated population, the fastest and slowest growth mutants (positive and negative growth, PMU and NMU, respectively) were selected, and the two mutants and the wild strain (WT) were subjected to transcriptome profiling with the goal of understanding the physiological mechanisms underlining fast growth behavior.

2 MATERIAL AND METHOD

2.1 *N. oceanica* and its culture

N. oceanica was obtained from Key Laboratory of Mariculture of Chinese Ministry of Education, Ocean University of China. The alga was cultured in *f*/2 medium (pH 7.8, salinity 30; Guillard and Ryther, 1962; Guillard, 1975). The *f*/2 medium was prepared with filtrated seawater, which was autoclaved at 121°C for 30 min. The alga was cultured at a constant temperature of 26°C and under 70 μmol photons/(m^2·s) following a 12 h/12 h light/dark regime.

2.2 MNNG mutation and mutant selection

Algal cells in the exponential growth phase were collected and washed twice with PBS (pH 7.2–7.4), resuspended and adjusted to 10^7 cells/mL in PBS, and subjected to 3.5 mg/mL MNNG mutation at room temperature (~25°C) for 1 h. The cells were then washed with PBS, resuspended in *f*/2 medium, and incubated in darkness overnight before being spread on *f*/2 solid medium (Nečas, 1975; Lee and Jones, 1976). One month later, clear and well-separated colonies were selected and cultured to the stationary growth phase on 24-well plates, one colony in each well.

WT cultures at the stationary phase were diluted to various degrees while monitoring the OD_{680} and the dilutions' cell density measured to build an OD_{680}/cell density curve. At different initial OD_{680} values (0.001 4, 0.007 0, and 0.035 0), WT suspensions were batch cultured in multiple flasks for each dilution in *f*/2 medium (20 mL inoculum in a 100-mL conical flask), with the OD_{680} measured every other day, one flask each time. Individual colonies were inoculated onto 24-well plates and cultured in *f*/2 medium to stationary phase, at which point each was inoculated into new flasks (initial OD_{680} 0.001 4–0.035 0) and batch cultured as with the WT cultures.

2.3 RNA extraction and transcriptome sequencing

Cells were harvested at the exponential growth

phase, which was on day 12 for WT and days 10 and 14 for positive and negative cells, respectively, by centrifugation at 5 000×*g* for 7 min and immediately frozen in liquid nitrogen for RNA extraction. Total RNA of each mutant and WT was extracted using TRIZOL reagent (Invitrogen Corp., Carlsbad, CA, USA), following the manufacturer's instructions. RNA degradation and genomic DNA contamination were evaluated through 1% agarose gel electrophoresis. RNA purity was evaluated using a NanoPhotometer® (Implen GmbH, Munchen, Germany). RNA concentration was measured using a Qubit® RNA Assay Kit in Qubit® 2.0 Fluorometer (Life Technologies, Inc., Carlsbad, CA, USA). RNA integrity was assessed using an RNA Nano 6000 Assay Kit of the Agilent Bioanalyzer 2100 System (Agilent Technologies, Inc., CA, USA). The 3′ poly(A)-tailed mRNA was isolated from the total RNA using oligo (dT)-linked magnetic beads (Oligotex mRNA Kits, Qiagen GmbH, Hilden, Germany), following manufacturer's instructions, then fragmented, and used as template for first-strand cDNA synthesis with reverse transcriptase and random hexamers. The second-strand cDNA was synthesized using RNase H and DNA polymerase I. After polishing the cDNA ends using T4 DNA polymerase and Klenow DNA polymerase at 20°C for 30 min, a single adenine base was added to the cDNA 3′-ends. Illumina mRNA-Seq Kit specific adaptors (Illumina Inc., San Diego, CA, USA) were then ligated to the resulting 3′-ends. The modified cDNA was gel purified and PCR amplified, yielding a cDNA library the size and concentration of which was determined on an Agilent 2100 Bioanalyzer (Agilent Technologies, Inc.). The cDNA library was sequenced commercially with an Illumina HiSeq 2000 Sequencer (Beijing Novogene Bioinformatics Technology Co., Ltd. Beijing, China).

2.4 Data processing

After removing low quality sequencing reads, clean reads were assembled using Trinity (Grabherr et al., 2011) by setting the minimum_kmer_coverage at 2 and other parameters at default. Gene functions were annotated by referring to NCBI non-redundant protein sequences (Nr), NCBI non-redundant nucleotide sequences (Nt), protein family (Pfam), clusters of orthologous groups of proteins (KOG/COG), a manually annotated and reviewed protein sequence database (Swiss-Prot), KEGG ortholog (KO), and gene ontology (GO).

The abundance of gene transcripts was determined using RSEM (Li and Dewey, 2011). Clean reads were stacked onto the assembled transcriptome and each counted for its gene number. The reads were normalized using the expected number of fragments per kilobase of transcript sequence per millions base pairs sequenced (FPKM), which avoided the effects of sequencing depth and transcript length (Trapnell et al., 2010). The read counts were adjusted using the edgeR software package with one scaling normalizing factor. Differential expression of any two samples was analyzed using the DEGseq (2010) R package. The *P*-value was adjusted using *q*-value software (Storey and Tibshirani, 2003). The differential expression was considered significant if *q*-value was <0.005 and $\log_2|\text{foldchange}|>1$.

Differentially expressed genes (DEGs) were enriched in Gene Ontology (GO) terms with the GOseq R software package, based on Wallenius' noncentral hypergeometric distribution (Young et al., 2010), which can avoid length bias in DEGs. KEGG (Kanehisa et al., 2008; http://www.genome.jp/kegg/), a database that aids in understanding the high-level functions and utility of biological systems, and KOBAS software (Mao et al., 2005) were used for enriching DEGs into KEGG pathways.

3 RESULT

3.1 Selection of fast and slow growth mutants

The WT cell density was found to be linearly proportional to its OD_{680} (R^2=0.999); such linearity also existed among the mutated strains (Fig.1a). The OD_{680} of these suspensions might have been associated with a range of cell characteristics, such as cell size and cell growth phase. However, the cell number of a cell line should be the principle factor associated with OD_{680}. WT and the mutant strains were cultured to stationary phase, diluted to different cell densities (OD_{680} of 0.001 4, 0.007 0, and 0.035 0), and cultured to obtain growth curves with different initial concentrations. The slope of these observed growth curves in exponential growth phase were found to be slightly different among the mutants but, fortunately, their final OD_{680} values were almost identical (Fig.1b). These findings allowed the identification of fast and slow growing strains according to their OD_{680} at stationary phase. Comparison of the final OD_{680} values of WT and 3 faster and 3 slower growing mutants obtained in triplicate, parallel mutation trials (Fig.1c) showed that they were OD_{680} values were

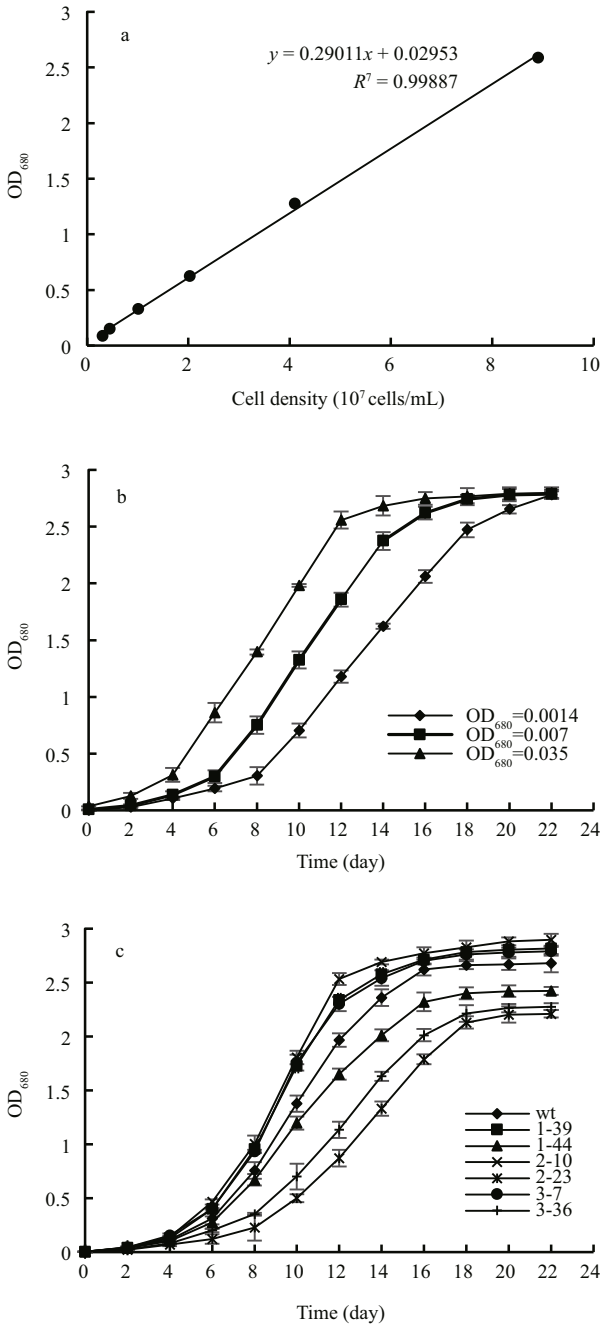

Fig.1 Growth curves of WT and six other strains (three faster and three slower) obtained through chemical mutation

a. linear relationship between cell density and OD_{680}; b. growth curve of WT inoculated at different initial OD_{680}'s; c. growth curves of WT and six mutants.

proportional to their cell density. The algal colonies were inoculated into multiple well plates, cultured to stationary phase, and transferred into *f*/2 medium in batch culture flasks. The initial OD_{680} might vary between cultures, but identical final OD_{680} values should be reached by stationary phase. According to this understanding, 3 faster (1-39, 2-10, and 3-7) and 3 slower (1-44, 2-23, and 3-36) growing mutants were selected from 153 mutants (clear and well-separated from other colonies) obtained from 3 mutation trials. After comparison, 2-10 and 2-23 were selected as the fastest and slowest growing mutants (PMU and NMU), respectively (Fig.1c).

Table 1 Number of unigenes functionally annotated against 7 available databases

Database	No. of unigenes	Percentage (%)
NR	15 129	45.42
NT	4 241	12.73
KO	6 232	18.71
SwissProt	9 892	29.69
PFAM	12 877	38.66
GO	12 975	38.95
KOG	7 166	21.51
All databases	1 544	4.63
At least 1 database	19 051	57.19
Total	33 307	100.00

3.2 RNA sequencing of WT and mutants

RNA sequencing was carried out for WT, PMU, and NMU. The frequencies of fragments normalized to FPKM distributed normally and were similar among WT, PMU, and NMU. In total, 147 241 944 clean reads were obtained from the three libraries. These reads were pooled for assembling transcripts, with a total of 33 307 unigenes (FPKM>0.3, mainly 15–60 bp) assembled and ranging from 16 425–201 bp in length with an average of 743 bp; the N50 length was 1 230 bp. Of 33 307 unigenes, 19 051 were annotated against at least one available database (Table 1) and assigned into function classifications of GO, KOG, and KEGG (Fig.2). In total, 19 611 unigenes were shared by WT, PMU, and NMU, with 1 121, 1 347, and 3 839 unigenes specific for WT, PMU, and NMU, respectively.

3.3 Difference among libraries

Between PMU and WT, 62 DEGs were detected (Fig.3) and, of these, 13 and 49 were upregulated and downregulated, respectively. Between PMU and WT, no DEG was significantly categorized into GO terms, and only the peroxisome pathway was enriched (Table 2, Fig.4a). Focusing on the direction of regulatory changes, it was found that the KEGG pathways of fatty acid metabolism and peroxisome were downregulated (Table 3). Among proteins

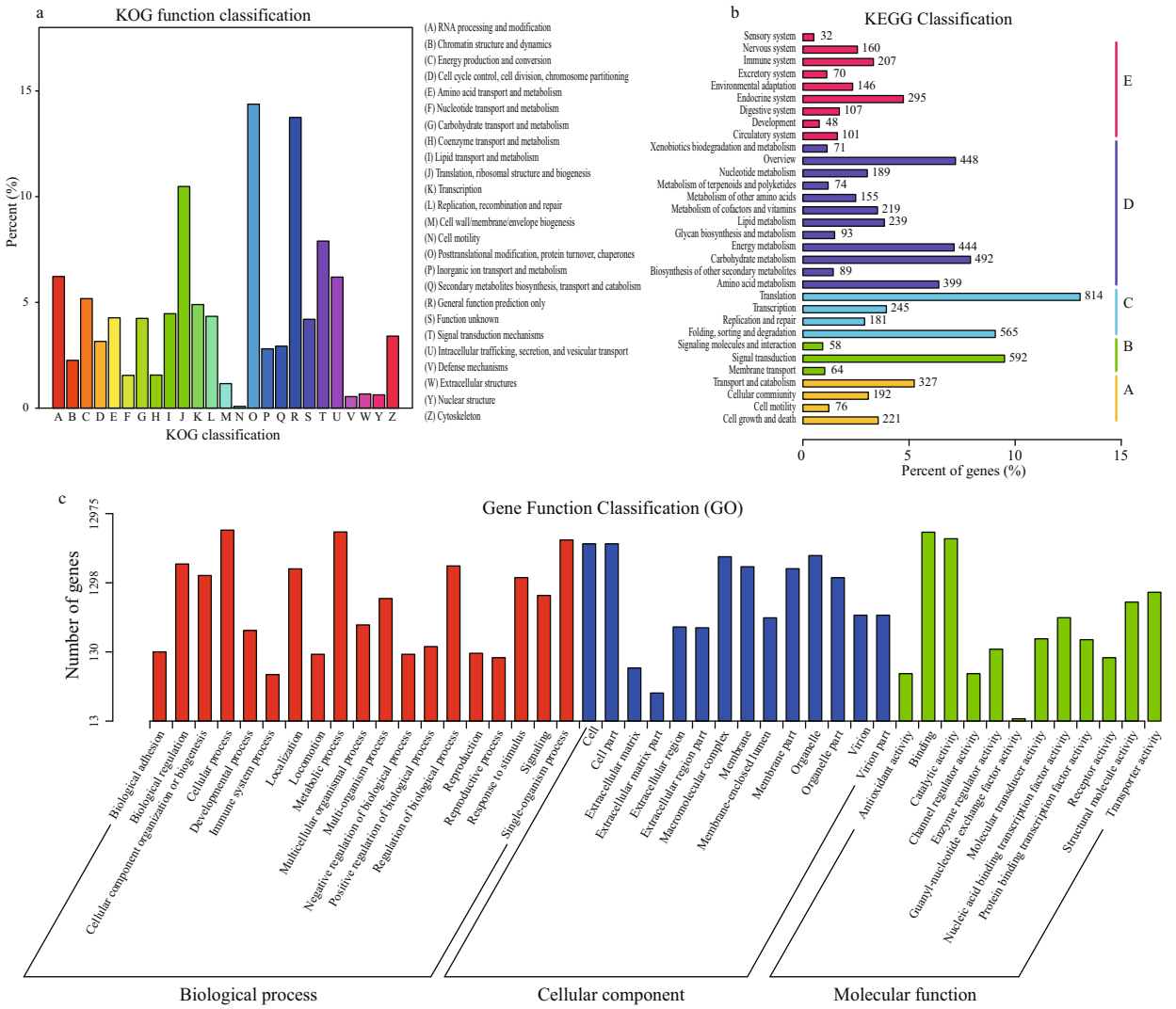

Fig.2 Functional assignment of annotated unigenes into KOG classifications (a), KEGG pathways (b), and GO terms (c)

In (b), five function categories: cellular processes, environmental information processing, genetic information processing, metabolism, and organismal systems (A–E, respectively).

encoded by these DEGs, $ELOVL_6$ limits C_{12}–C_{16} fatty acid elongation and ACSL degrades C_{12}–C_{22} fatty acids and synthesizes acyl-CoA. Downregulation of their encoding genes indicated that fatty acid synthesis was decreased in PMU. The observed DEGs also included genes encoding MCM_2, a member of the MCM family, which functions as a six-polymer complex in DNA prereplication, allowing cells to enter S phase, and $PSMD_1$, a part of the proteasome, which participates in ubiquitin-mediated proteolysis, ensuring normal running of the cell cycle. Upregulation of genes encoding MCM_2 and $PSMD_1$ observed here might have indicated acceleration of cell division and enhancement of cell cycling by PMU.

Between WT and NMU, 1428 DEGs were identified (Fig.3) and, of them, 633 and 795 were upregulated and downregulated, respectively. Between WT and NMU, KEGG pathways of ribosome and fatty acid metabolism were significantly enriched (Table 4, Fig.4b). Focusing on the direction of regulation, upregulated KEGG pathways included biosynthesis of amino acids, fatty acids, pigments, ribosome, and photosynthetic elements (Table 5). NMU cells divided more slowly than those of WT and showed four DEGs (encoding MCM_2, SCF, SMC_3, and ATM/ATR) involved in the cell cycle that were downregulated. These downregulated genes were inferred to suggest a closing of the avenue for transitioning from the G_1 phase to S phase but, instead, promoted the synthesis of amino acids, fatty acids, and pigments as well as construction of ribosomes and photosynthetic machinery.

Comparison of PMU with NMU demonstrated the differential expression of 1 901 unigenes (Fig.3) and,

Table 2 GO terms enriched significantly by DEGs

DEGs between/GO term	Term description	No. of DEGs	No. of genes in term	Enrichment factor	Corrected *P*-value
		NMU and WT*			
GO:0008152	Metabolic process	641	7 286	0.088	0.020
GO:0009058	Biosynthetic process	347	3 630	0.096	0.042
GO:0032991	Macromolecular complex	278	2 991	0.093	0.015
GO:0019538	Protein metabolic process	235	2 375	0.099	0.010
GO:0005737	Cytoplasm	218	2 160	0.101	0.000
GO:0044267	Cellular protein metabolic process	190	1 891	0.101	0.002
GO:0044444	Cytoplasmic part	189	1 726	0.1105	0.000
GO:0043228	Non-membrane-bounded organelle	168	1 459	0.115	0.000
GO:0043232	Intracellular non-membrane-bounded organelle	168	1 459	0.115	0.000
GO:0016491	Oxidoreductase activity	164	1 271	0.129	0.000
GO:0055114	Oxidation-reduction process	157	1 288	0.122	0.006
GO:0071840	Cellular component organization biogenesis	157	1 620	0.097	0.022
GO:0030529	Ribonucleoprotein complex	122	906	0.135	0.000
GO:0044085	Cellular component biogenesis	119	1 014	0.117	0.000
GO:0005198	Structural molecule activity	112	876	0.128	0.000
GO:0006412	Translation	108	815	0.133	0.000
GO:0005840	Ribosome	101	716	0.141	0.000
GO:0042254	Ribosome biogenesis	100	734	0.136	0.000
GO:0022613	Ribonucleoprotein complex biogenesis	100	742	0.135	0.000
GO:0003735	Structural constituent of ribosome	94	619	0.152	0.000
GO:0048037	Cofactor binding	73	436	0.167	0.026
GO:0050662	Coenzyme binding	58	326	0.178	0.040
GO:0032787	Monocarboxylic acid metabolic process	38	204	0.186	0.040
		PMU and NMU			
GO:0008152	Metabolic process	867	7 286	0.119	0.005
GO:0005622	Intracellular	523	4 497	0.116	0.035
GO:0044424	Intracellular part	508	4 326	0.117	0.010
GO:0044710	Single-organism metabolic process	411	2 845	0.145	0.013
GO:0032991	Macromolecular complex	374	2 991	0.125	0.001
GO:0005737	Cytoplasm	294	2 160	0.136	0.000
GO:0044444	Cytoplasmic part	248	1 726	0.144	0.000
GO:0044267	Cellular protein metabolic process	240	1 891	0.127	0.020
GO:0016491	Oxidoreductase activity	225	1 271	0.177	0.000
GO:0055114	Oxidation-reduction process	221	1 288	0.172	0.000
GO:0043228	Non-membrane-bounded organelle	201	1 459	0.138	0.000
GO:0043232	Intracellular non-membrane-bounded organelle	201	1 459	0.138	0.000
GO:0044085	Cellular component biogenesis	137	1 014	0.135	0.001
GO:0030529	Ribonucleoprotein complex	136	906	0.150	0.000
GO:0005198	Structural molecule activity	123	876	0.140	0.001
GO:0006412	Translation	121	815	0.149	0.000
GO:0005840	Ribosome	108	716	0.151	0.000
GO:0042254	Ribosome biogenesis	108	734	0.147	0.000
GO:0022613	Ribonucleoprotein complex biogenesis	108	742	0.146	0.000
GO:0003735	Structural constituent of ribosome	98	619	0.158	0.000
GO:0048037	Cofactor binding	93	436	0.213	0.023
GO:0050662	Coenzyme binding	77	326	0.236	0.007
GO:0006091	Generation of precursor metabolites and energy	64	353	0.181	0.002
GO:0006457	Protein folding	33	170	0.194	0.005
GO:0070469	Respiratory chain	14	50	0.280	0.022
GO:0019203	Carbohydrate phosphatase activity	8	12	0.667	0.022
GO:0042132	Fructose 1,6-bisphosphate-1-phosphatasse activity	8	12	0.667	0.022
GO:0050308	Sugar-phosphatase activity	8	12	0.667	0.022

*: no GO term enriched between PMU and WT.

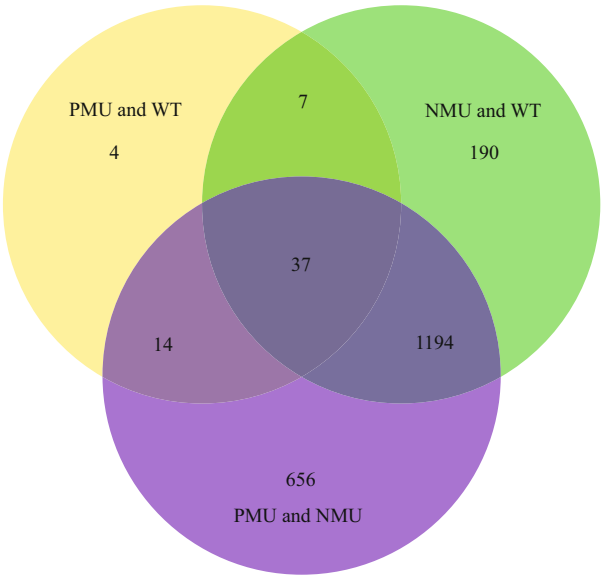

Fig.3 Venn diagram of DEGs between PMU and WT, NMU and WT, and PMU and NMU (yellow, green, and purple, respectively)

of them, 1 014 and 887 were upregulated and downregulated, respectively. The only KEGG pathway enriched by these DEGs was fatty acid metabolism (Table 4, Fig.4c), in which 11 and 15 genes were upregulated and downregulated, respectively. DEGs for fatty acid biosynthesis showed downregulation while those for fatty acid degradation showed upregulation. Fatty acid degradation yields acetyl-CoA and small intermediate molecules that might enter the tricarboxylic acid cycle and oxidative phosphorylation, generating ATP. In total, 12 DEGs involved in the cell cycle were upregulated, the relationships of which are shown in Figure 5. Downregulated DEGs also included genes responsible for the degradation of amino acids, fatty acids, pigments, and sugar, and construction of ribosome and photosynthetic machinery (Table 3). These findings suggested the negation of the conjectures that (1) fast growth was controlled by genes functioning in cell cycle and (2) cells grew faster by reducing synthesis of amino acids, fatty acids, and sugar, as well as construction of ribosome and photosynthesis machinery.

4 DISCUSSION

By profiling and comparing the transcriptome of the WT and two mutant strains, it was found that *Nannochloropsis* cells divided and thus grew more rapidly by downregulating the pathways of peroxisome and fatty acid metabolism, and

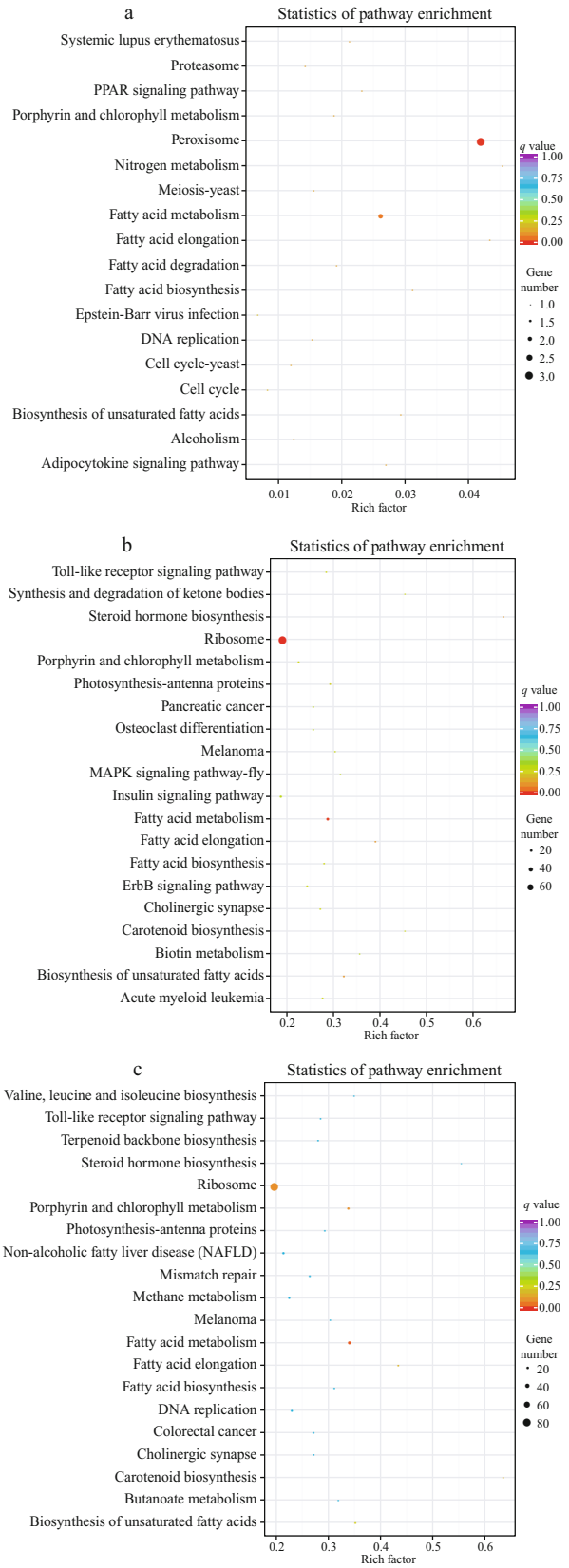

Fig.4 DEGs between PMU and WT, NMU and WT, and PMU and NMU (a–c, respectively) enriched in KEGG pathways

Table 3 Downregulated KEGG pathways enriched significantly by downregulated DEGs

DEGs between/KEGG term	Term description	No. of DEGs	No. of genes in term	Enrichment factor	Corrected *P*-value
		PMU and WT*			
ko01212	Fatty acid metabolism	2	76	0.026	0.016
ko04146	Peroxisome	3	71	0.042	0.001
PMU and NMU					
ko00970	Aminoacyl-*t*-RNA biosynthesis	13	75	0.173	0.011
ko01230	Amino acid biosynthesis	29	232	0.125	0.002
ko01040	Unsaturated fatty acid biosynthesis	9	34	0.265	0.007
ko00780	Biotin metabolism	5	14	0.357	0.023
ko00710	Carbon fixation in photosynthetic organisms	15	94	0.160	0.010
ko01200	Carbon metabolism	26	259	0.100	0.029
ko00906	Carotenoid biosynthesis	5	11	0.455	0.014
ko00061	Fatty acid biosynthesis	7	32	0.219	0.029
ko00062	Fatty acid elongation	7	23	0.304	0.012
ko01212	Fatty acid metabolism	15	76	0.197	0.002
ko00010	Glycolysis/gluconeogenesis	20	129	0.155	0.002
ko05016	Huntington's disease	17	136	0.125	0.023
ko04932	Non-alcoholic fatty liver disease	12	79	0.152	0.023
ko00190	Oxidative phosphorylation	18	143	0.126	0.022
ko05012	Parkinson's disease	15	109	0.138	0.022
ko00030	Pentose phosphate pathway	10	50	0.200	0.014
ko00195	Photosynthesis	9	53	0.170	0.034
ko00196	Photosynthetic antenna proteins	10	34	0.294	0.002
ko00860	Porphyrin and chlorophyll metabolism	16	53	0.302	0.000
ko03010	Ribosome	81	406	0.200	0.000
ko00521	Streptomycin biosynthesis	5	14	0.357	0.023
ko00920	Sulfur metabolism	6	26	0.231	0.040
ko00900	Terpenoid backbone biosynthesis	7	32	0.219	0.029

*: no KEGG pathway downregulated between NMU and WT.

Table 4 KEGG pathways enriched significantly by all DEGs

DEGs between/KEGG term	Term description	No. of DEGs	No. of genes in term	Enrichment factor	Corrected *P*-value
		PMU and WT			
ko04146	Peroxisome	3	71	0.042	0.004
		NMU and WT			
ko03010	Ribosome	79	406	0.195	0.000
ko01212	Fatty acid metabolism	22	76	0.290	0.010
		PMU and NMU			
ko01212	Fatty acid metabolism	26	76	0.342	0.023

upregulating gene expression involved in cell division and cycling. These conclusions were supported by the NMU, which showed upregulated biosynthesis of amino acids, fatty acids, pigments, photosynthetic elements, and ribosome, while downregulating genes were involved in cell cycling. Direct comparison between the PMU and NMU indicated that, in PMU, fatty acid biosynthesis was downregulated while fatty

Table 5 Upregulated KEGG pathways enriched significantly by upregulated DEGs

DEGs between/KEGG term	Term description	No. of DEGs	No. of genes in term	Enrichment factor	Corrected *P*-value
		NMU and WT*			
ko01230	Amino acid biosynthesis	22	232	0.095	0.007
ko01040	Unsaturated fatty acid biosynthesis	8	34	0.235	0.004
ko00780	Biotin metabolism	5	14	0.357	0.011
ko00062	Fatty acid elongation	7	23	0.304	0.004
ko01212	Fatty acid metabolism	12	76	0.158	0.004
ko00195	Photosynthesis	9	53	0.170	0.011
ko00196	Photosynthesis - antenna proteins	10	34	0.294	0.000
ko00860	Porphyrin and chlorophyll metabolism	11	53	0.208	0.002
ko03010	Ribosome	79	406	0.195	0.000
ko00920	Sulfur metabolism	6	26	0.231	0.019
ko00290	Valine, leucine and isoleucine biosynthesis	5	20	0.250	0.033

*: no KEGG pathway upregulated between PMU and WT, and PMU and NMU.

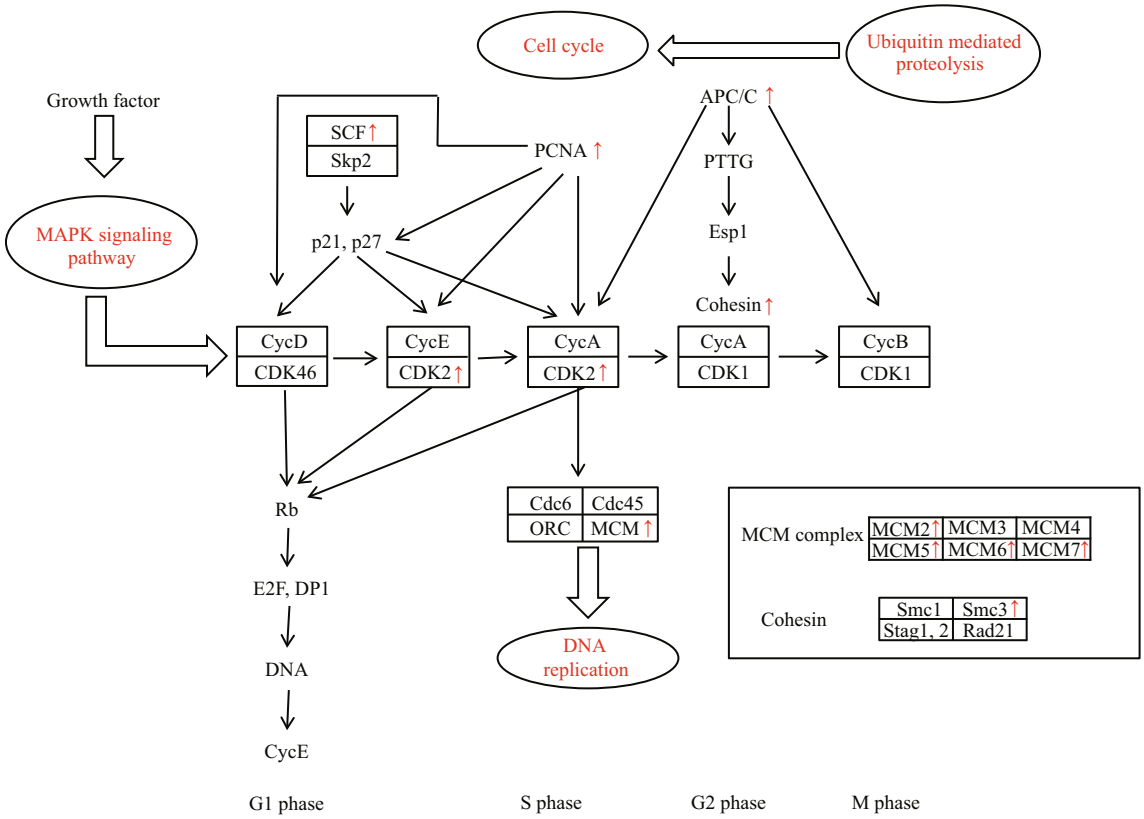

Fig.5 Upregulated expression of genes encoding key proteins (red arrows) involved in cell cycle identified by comparing DEGs between PMU and NMU. CDK, cyclin dependent kinase

Cyc: cyclin; MCM: minichromosome maintenance; Cohesin: protein complex regulating sister chromatid separation during cell division; PCNA: proliferating cell nuclear antigen; SCF: stem cell factor; and APC/C: anaphase-promoting complex.

acid degradation was upregulated. In PMU, downregulated genes also included genes responsible for metabolism of amino acids, fatty acids, pigments, and sugar as well as photosynthesis and ribosome assembly. These observations also indicated that 12 DEGs functioning in the cell cycle were upregulated. Thus, it was concluded here that *Nannochloropsis* cells grew faster by upregulating expression of genes functioning in the cell cycle and downregulating genes involved in synthesis of amino acids, fatty

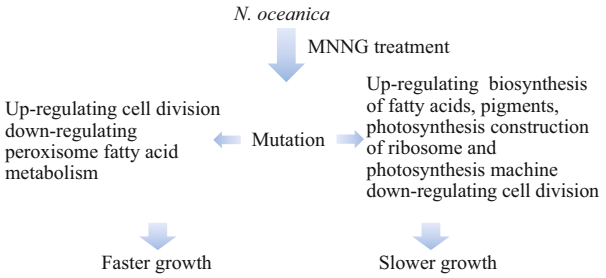

Fig.6 Possible association between MNNG mutation and growth performance of *N. oceanica*

acids, and sugar as well as construction of ribosome and photosynthetic machinery (Fig.6). However, the relationship among genes responsible for cell cycle, metabolism of fatty acids, amino acids among others, and construction of ribosome and photosynthetic machinery remain unclear. Further studies, such as genetic investigations, are required for clarifying the genetic (and thus metabolic) networks underlining the growth performance of *Nannochloropsis*.

Except for those mutations generated occasionally during DNA replication, DNA can be mutated through diverse natural and artificial methods that include traditional chemical and physical methods as well as some newly developed and widely practiced methods, for example, atmospheric and room temperature plasma (ARTP; Zhang et al., 2014) and low-energy heavy ion beam implantation (Tang and Yu, 2007; Zhang and Yu, 2009). The effects of these methods on DNA differ. In this study, the effectiveness of MNNG mutation was illustrated, but this success did not indicate that MNNG mutation was the most appropriate or applicable method. This study explored a means of creating and breeding microalgal strains, particularly species possessing a monoploid genome and asexual reproduction, such as does *Nannochloropsis*. In future studies, *Nannochloropsis* will be mutated by other methods, with the goal of breeding elite strains for maximal production and to develop various interesting strains for genetic studies.

For microalgae, various strategies have been applied for their genetic improvement. For less studied microalgal species, such as *Nannochloropsis*, new research tools should be developed for their improvement, as genetic transformation of *Nannochloropsis* has not met much success in most laboratories. Therefore, the identification or development of highly effective transformation tools for this species will promote its improvement and deciphering of its gene functions.

5 CONCLUSION

Based on MNNG mutation and transcriptome profiling, this method of mutation was shown to be effective for improving *Nannochloropsis* growth and that *Nannochloropsis* cells divided faster by downregulating pathways for peroxisome and fatty acid metabolism, while upregulating expression of genes involved in the cell cycle. Further research is required to determine the relationship among these observed changes.

References

Boussiba S, Vonshak A, Cohen Z, Avissar Y, Richmond A. 1987. Lipid and biomass production by the halotolerant microalga *Nannochloropsis salina*. *Biomass*, **12**(1): 37-47.

Chepurnov V A, Chaerle P, Roef L, Meirhaeghe A, Vanhoutte K. 2011. Classical breeding in diatoms: scientific background and practical perspectives. *In*: Seckbach J, Kociolek J P eds. The Diatom World. Springer, Netherlands. p.167-194.

Fang M Y, Jin L H, Zhang C, Tan Y Y, Jiang P X, Ge N, Li H P, Xing X H. 2013. Rapid mutation of *Spirulina platensis* by a new mutagenesis system of atmospheric and room temperature plasmas (ARTP) and generation of a mutant library with diverse phenotypes. *PLoS One*, **8**(10): e77046.

Gao C F, Wang Y, Shen Y, Yan D, He X, Dai J B, Wu Q Y. 2014. Oil accumulation mechanisms of the oleaginous microalga *Chlorella protothecoides* revealed through its genome, transcriptomes, and proteomes. *BMC Genomics*, **15**: 582.

Grabherr M G, Haas B J, Yassour M, Levin J Z, Thompson D A, Amit I, Adiconis X, Fan L, Raychowdhury R, Zeng Q D, Chen Z H, Mauceli E, Hacohen N, Gnirke A, Rhind N, di Palma F, Birren B W, Nusbaum C, Lindblad-Toh K, Friedman N, Regev A. 2011. Full-length transcriptome assembly from RNA-Seq data without a reference genome. *Nature Biotechnology*, **29**(7): 644-652.

Guillard R R L. 1975. Culture of phytoplankton for feeding marine invertebrates. *In*: Smith W L, Chanley M H eds. Culture of Marine Invertebrate Animals. Springer US, New York, America. p.29-60.

Guillard R R, Ryther J H. 1962. Studies of marine planktonic diatoms. I. *Cyclotella nana* Hustedt, and *Detonula confervacea* (Cleve) Gran. *Canadian Journal of Microbiology*, **8**(2): 229-239.

Guo L, Yang G P. 2015. The mechanism of the acclimation of *Nannochloropsis oceanica* to freshwater deduced from its transcriptome profiles. *Journal of Ocean University of China*, **14**(5): 922-930.

He M, Wang Y, Hua W P, Zhang Y, Wang Z Z. 2012. *De Novo* sequencing of *Hypericum perforatum* transcriptome to identify potential genes involved in the biosynthesis of

active metabolites. *PLoS One*, **7**(7): e42081.

Jinkerson R E, Jonikas M C. 2015. Molecular techniques to interrogate and edit the *Chlamydomonas* nuclear genome. *The Plant Journal*, **82**(3): 393-412.

Kanehisa M, Araki M, Goto S, Hattori M, Hirakawa M, Itoh M, Katayama T, Kawashima S, Okuda S, Tokimatsu T, Yamanishi Y. 2008. KEGG for linking genomes to life and the environment. *Nucleic Acids Research*, **36**(S1): D480-D484.

Kawata Y, Yamano N, Kojima H, Itoh S. 1991. Expression of salmon growth hormone in the cyanobacterium *Agmenellum quadruplicatum*. *Biotechnology Letters*, **13**(12): 851-856.

Kim S, Kim M J, Jung M G, Lee S, Baek Y S, Kang S H, Choi H G. 2013. De novo transcriptome analysis of an Arctic microalga, *Chlamydomonas* sp. *Genes & Genomics*, **35**(2): 215-223.

Lee R W, Jones R F. 1976. Lethal and mutagenic effects of nitrosoguanidine on synchronized *Chlamydomonas*. *Molecular and General Genetics*, **147**(3): 283-289.

Li B, Dewey C N. 2011. RSEM: accurate transcript quantification from RNA-Seq data with or without a reference genome. *BMC Bioinformatics*, **12**: 323.

Mao X Z, Cai T, Olyarchuk J G, Wei L P. 2005. Automated genome annotation and pathway identification using the KEGG Orthology (KO) as a controlled vocabulary. *Bioinformatics*, **21**(19): 3 787-3 793.

Mardis E R. 2008. The impact of next-generation sequencing technology on genetics. *Trends in Genetics*, **24**(3): 133-141.

Nečas J. 1975. Physiological and mutagenic effects of N-methyl-N'-nitro-N-nitrosoguanidine in populations of chlorococcal algae. *Biologia Plantarum*, **17**(2): 130-138.

Ortiz-Marquez J C F, Nascimento M D, Zehr J P, Curatti L. 2013. Genetic engineering of multispecies microbial cell factories as an alternative for bioenergy production. *Trends in Biotechnology*, **31**(9): 521-529.

Ouyang L L, Chen S H, Li Y, Zhou Z G. 2013. Transcriptome analysis reveals unique C4-like photosynthesis and oil body formation in an arachidonic acid-rich microalga *Myrmecia incisa* Reisigl H4301. *BMC Genomics*, **14**: 396.

Pan K H, Qin J J, Li S, Dai W K, Zhu B H, Jin Y C, Yu W G, Yang G P, Li D F. 2011. Nuclear monoploidy and asexual propagation of *Nannochloropsis oceanica* (eustigmatophyceae) as revealed by its genome sequence. *Journal of Phycology*, **47**(6): 1 425-1 432.

Petkov G, Ivanova A, Iliev A, Vaseva I. 2012. A critical look at the microalgae biodiesel. *European Journal of Lipid Science and Technology*, **114**(2): 103-111.

Rismani-Yazdi H, Haznedaroglu B Z, Hsin C, Peccia J. 2012. Transcriptomic analysis of the oleaginous microalga *Neochloris oleoabundans* reveals metabolic insights into triacylglyceride accumulation. *Biotechnology for Biofuels*, **5**(1): 74.

Storey J D, Tibshirani R. 2003. Statistical significance for genomewide studies. *Proceedings of the National Academy of Sciences of the United States of America*, **100**(16): 9 440-9 445.

Sukenik A, Carmeli Y, Berner T. 1989. Regulation of fatty acid composition by irradiance level in the Eustigmatophyte *Nannochloropsis* sp. *Journal of Phycology*, **25**(4): 686-692.

Takouridis S J, Tribe D E, Gras S L, Martin G J O. 2015. The selective breeding of the freshwater microalga *Chlamydomonas reinhardtii* for growth in salinity. *Bioresource Technology*, **184**: 18-22.

Tang M L, Yu Z L. 2007. Bioeffects of low energy ion beam implantation: DNA damage, mutation and gene transter. *Plasma Science and Technology*, **9**(4): 513-518.

Tilman D, Socolow R, Foley J A, Hill J, Larson E, Lynd L, Pacala S, Reilly J, Searchinger T, Somerville C, Williams R. 2009. Beneficial biofuels-the food, energy, and environment trilemma. *Science*, **325**(5938): 270-271.

Tjahjono A E, Kakizono T, Hayama Y, Nishio N, Nagai S. 1994. Isolation of resistant mutants against carotenoid biosynthesis inhibitors for a green alga *Haematococcus pluvialis*, and their hybrid formation by protoplast fusion for breeding of higher astaxanthin producers. *Journal of Fermentation and Bioengineering*, **77**(4): 352-357.

Trapnell C, Williams B A, Pertea G, Mortazavi A, Kwan G, van Baren M J, Salzberg S L, Wold B J, Pachter L. 2010. Transcript assembly and quantification by RNA-Seq reveals unannotated transcripts and isoform switching during cell differentiation. *Nature Biotechnology*, **28**(5): 511-515.

Wijffels R H, Barbosa M J. 2010. An outlook on microalgal biofuels. *Science*, **329**(5993): 796-799.

Xue J, Niu Y F, Huang T, Yang W D, Liu J S, Li H Y. 2015. Genetic improvement of the microalga *Phaeodactylum tricornutum* for boosting neutral lipid accumulation. *Metabolic Engineering*, **27**: 1-9.

Young M D, Wakefield M J, Smyth G K, Oshlack A. 2010. Gene ontology analysis for RNA-seq: accounting for selection bias. *Genome Biology*, **11**(2): R14.

Zhang D H, Lee Y K. 1997. Enhanced accumulation of secondary carotenoids in a mutant of the green alga, *Chlorococcum* sp. *Journal of Applied Phycology*, **9**(5): 459-463.

Zhang N, Yu L. 2009. Mutation breeding of β-carotene producing strain *B. trispora* by low energy ion implantation. *Plasma Science and Technology*, **11**(1): 110-115.

Zhang X, Zhang X F, Li H P, Wang L Y, Zhang C, Xing X H, Bao C Y. 2014. Atmospheric and room temperature plasma (ARTP) as a new powerful mutagenesis tool. *Applied Microbiology and Biotechnology*, **98**(12): 5 387-5 396.